Available online at www.sciencedirect.com
SCIENCE DIRECT
Catalysis Today 105 (2005) 362–366
CATALYSIS TODAY
www.elsevier.com/locate/cattod

# Performance of a catalytic membrane reactor for the Fischer–Tropsch synthesis

A.A. Khassin *, A.G. Sipatrov, T.M. Yurieva, G.K. Chermashentseva, N.A. Rudina, V.N. Parmon

*Boreskov Institute of Catalysis, 5, Pr. Lavrentieva, Novosibirsk 630090, Russia*

Available online 11 July 2005

**Abstract**

The study of permeable composite monolith (PCM) membranes for the Fischer–Tropsch synthesis is continued. On the scale of membranes with outer diameter of 42 mm, it is proved that PCM can combine high productivity of hydrocarbons (>55 $kg_{C_{5+}}$ $(m^3_{PCM}\ h)^{-1}$ at 0.6 MPa, 484 K), high selectivity towards heavy hydrocarbons ($\alpha_{ASF} > 0.85$, $C_{5+}$ upto 0.9) as well as high heat-conductivity and high mechanical strength.


*Keywords:* Fischer–Tropsch synthesis; Membrane reactor; Composite; Monolith

## 1. Introduction

In some recent publications [1–3], the catalytic membrane reactors are discussed as a prospective approach for Fischer–Tropsch synthesis (FTS) catalyst bed scheme. Among them are those [1,2] using permeable composite monoliths (PCM). These studies were performed using small membranes of different pore structure and shape, with geometric volume of 2 $cm^3$. The use of PCM was supposed as helpful in solving the knotty problem of trade between high concentration of the active component and diffusion limitations, which hinders chemical engineers from improving the productivity of the traditional reactor designs [4].

The present paper illustrates the possibility of achieving high productivity and selectivity of the Fischer–Tropsch synthesis at small temperature gradient and low pressure drop using the PCM membranes with the diameter close to that of the industrial tubular fixed bed (ARGE-type) reactor.

## 2. Experimental

### 2.1. PCM membrane preparation

The PCM membrane was prepared according to the patent [5] in three following steps: (1) mixing of the powders of the Co-Al co-precipitated catalyst, a pore-producing agent and dendritic metallic copper powder as a reinforcing heat-conductive agent; (2) pressing the mixture into a hollow cylinder; (3) calcination in the inert gas flow and then in the flowing hydrogen at 620 °C.

Finally, the PCM membrane is a strong three-modal porous structure, which is permeated by the syngas (see Fig. 1). The pores with the effective radius >2–3 μm are almost gas-filled and are responsible for the gas permeation (“transport pores”). The smaller pores are flooded with liquid products due to capillary forces and are not permeable. The most narrow pores (effective radius less than 0.5 μm) are located inside the catalyst particles and the mass transfer within these pores is accounted for by the molecular diffusion. The pore structure parameters depend on the preparation conditions, such as the mean particle size of the initial powders, pressing force, regimes of the calcination and reduction.

* Corresponding author. Tel.: +7 383 330 91 09; fax: +7 383 330 80 56.
*E-mail address:* aakhassin@catalysis.ru (A.A. Khassin).

0920-5861/$ – see front matter 
doi:10.1016/j.cattod.2005.06.031

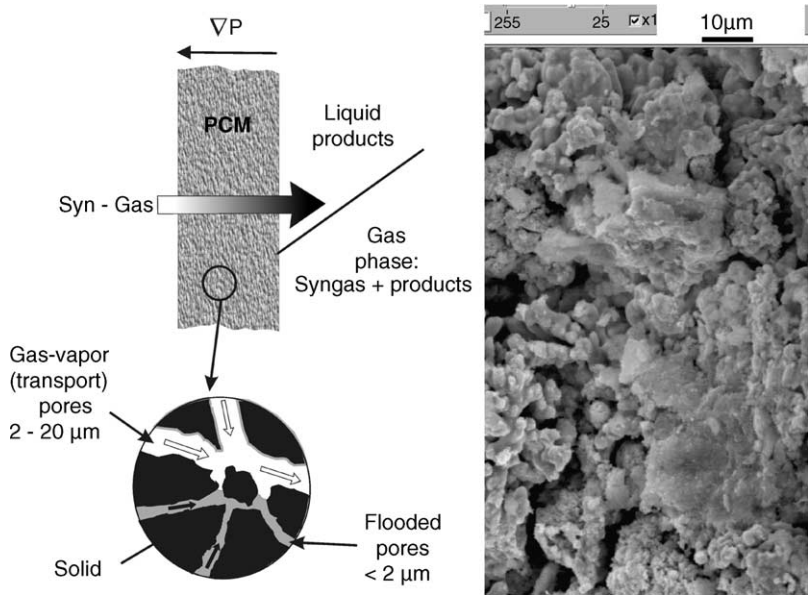


Fig. 1. The scheme of the PCM membrane pore structure and a typical SEM image of PCM.

The details of the PCM porous structure characterization and the discussion on the effect of the pore structure parameters on the PCM catalytic performance in the FTS were reported earlier in Refs. [1,2]. In these publications, the criteria of the optimal pore distribution by size were formulated. By varying the preparation conditions and the PCM composition, it is possible to change the pore-size distribution of the membrane and so to change the performance of the PCM in the Fischer–Tropsch synthesis. The width of the transport pores distribution by size impacts to the extent of the gas flow bypass and the extensiveness of the stagnation zones. Therefore, the productivity is favored at narrow distribution of the pores by size. The concentration of transport pores affects the mean distance between two adjacent transport pores, and so, the intraparticle diffusion constraints can be weakened by increasing the transport pores concentration. After taking into account these correlations, it becomes evident that the most efficient PCM membrane should have high concentration of the transport pores having similar size [1,2]. With respect to these studies, the ‘‘optimal’’ membranes were prepared using the preparation conditions close to that of PCM–Cyl-3 of the cited paper; PCM17 having outer diameter of ca. 17 mm and the diameter of the axial hole of ca. 7 mm and PCM42 with diameters of ca. 42 and 9 mm, correspondingly.

Fig. 2 shows the density functions of the pore-size distributions estimated by using the bubble point method. The distribution of pores is wider for PCM42. This should bring about stronger difference in the gas residence time and somewhat worse performance of the membrane. According to Hagen–Poiseuille equation, the almost two-fold difference in the PCM42 pore-sizes should cause a difference in residence time by a factor of more than 14. Table 1 gives the geometric and pore structure parameters of the membranes.

### 2.2. Catalytic studies

The catalytic properties of the PCM membranes were studied in a radial flow membrane reactor at 484 ± 1 K at 0.1 and 0.6 MPa and the inlet gas composition $H_2$:CO:$N_2$ = 6:3:1 (v/v/v). The outlet gas composition was measured by two GCs; CO, $H_2$, $N_2$ and $CH_4$ were separated by the packed column with activated carbon and detected by TCD, while the $C_1$–$C_8$ hydrocarbons were separated by a γ-alumina packed column and detected by FID. Liquid hydrocarbons were condensed at 20 °C and analyzed by using the capillary SE-30 column and FID.

The principle scheme of the PCM radial flow membrane reactor used is given by Fig. 3. Normally, the gas was fed into the central void of the cylinder, then permeated through membrane and escaped from the outer surface. It is noteworthy that the direction of the gas flow has a significant

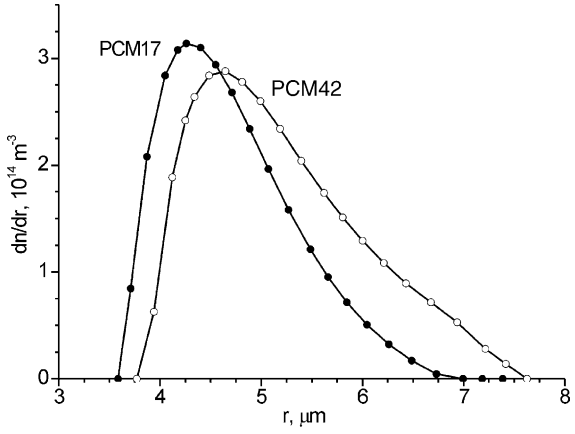


Fig. 2. The estimated density functions of the transport pore by size distributions for the PCM membranes under the study.

Table 1
The geometric and pore structure parameters of the PCM membranes under the study

| Sample | $D_{out}$ (mm) | $D_{in}$ (mm) | $H_{PCM}$ (mm) | $\rho_{cat}$ (g cm$^{-3}$) | $h_{insul}$ (mm) | $r_{max}$ (μm) | $r_{average}$ (μm) | $\delta$ (μm) | $K$ (mDarcy) |
|---|---|---|---|---|---|---|---|---|---|
| PCM17 | 17 | 7 | 9 | 0.85 | 1.5 | 7.0 | 4.8 | 1.45 | 120 |
| PCM42 | 42.3 | 9.5 | 16.6 | 0.90 | 2.5 | 7.6 | 5.0 | 1.80 | 137 |

$D_{out}$, $D_{in}$ and $H_{PCM}$—outer diameter, inner diameter and height of the PCM membrane, respectively; $\rho_{cat}$—the catalyst loading density; $h_{insul}$—thickness of the porous copper insulating layers; $r_{max}$ and $r_{average}$—maximal and average pore radii, respectively; $\delta$—halfwidth of the pore-size distribution; $K$—permeability.

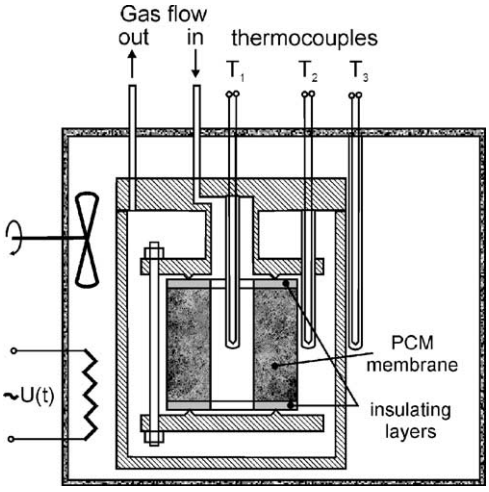


Fig. 3. The scheme of the radial flow catalytic membrane reactor used for the FT synthesis.

impact on the PCM performance in the FTS [2]. The in-to-out direction was selected for the present study, since it provides higher productivity of the PCM membrane. Reactor temperature was measured by two thermocouples in the PCM center and in the gas phase near the outer surface of the PCM. Another thermocouple was used for measuring the temperature in the thermostat outside the reactor case.

## 3. Results and discussion

Table 2 shows the results of the catalytic tests of the sample PCM17 in the Fischer–Tropsch synthesis at 483 K, 0.1 MPa, $H_2$:CO = 2 at different gas flow as a function of the CO conversion extent. The data presented were measured after 8 h from each change of the reaction conditions. The observed drop of the CO and $H_2$ conversions during the first few hours is due to the saturation of the reaction system with reactants. The catalyst deactivation during the next 60 h was approximately 3–4%, as it was proved by the additional long tests at the syngas flow of 19.3 mmol ($g_{cat}$ h)$^{-1}$ (resulting in 62% of CO conversion, productivity of 52 mg ($g_{cat}$ h)$^{-1}$).

Taking into account the high catalyst loading (0.85 g cm$^{-3}$ for the PCM under discussion), one can see that even at 0.1 MPa, the PCM17 membrane provides the space–time yield (STY) of liquid hydrocarbons >27 $mg_{C_{5+}}$ (cm$^3$ h)$^{-1}$, where the exterior volume of the membrane is considered. Meanwhile, this value is close to the space–time yield of the slurry bed reactor operating at 2 MPa (e.g. SASOL SSPD [6]). At low conversions, the STY $C_{5+}$ exceeds 40 $mg_{C_{5+}}$ (cm$^3$ h)$^{-1}$. At that, the value of the Anderson–Schulz–Flory distribution parameter $\alpha_{ASF}$ for the fraction of $C_{10+}$ is >0.85.

The activity of the PCM42 membrane at 0.1 MPa is worse than that of PCM17 described above. This is, most probably, due to a wider pore-size distribution (see Fig. 2), which resulted in bypass through wide pores and flow stagnation in the narrow ones. Also the same reason accounts for the lower $\alpha_{ASF}$ parameter value and lower olefins content for the PCM42 membrane. The reason of lower selectivity towards methane and ethane is not yet well understood.

Table 2
The catalytic data for the PCM membranes in the Fischer–Tropsch synthesis

| | | | | |
|---|---|---|---|---|
| PCM17, $H_2$:$CO_{inlet}$ = 2, $T$ = 484 K, $P$ = 0.1 MPa | | | | |
| Gas flow, $V_g$, $mmol_g$ ($g_{cat}$ h)$^{-1}$ | 19.3 | 40.1 | 80.4 | 161 |
| CO conversion extent, $X_{CO}$ (%) | 64.1 | 40.0 | 28.9 | 11.6 |
| $H_2$ conversion extent, $X_{H_2}$ (%) | 69.4 | 46.6 | 34.7 | 14.2 |
| $H_2$:CO outlet ratio | 1.70 | 1.78 | 1.83 | 1.94 |
| Productivity, $mg_{HC}$ ($g_{cat}$ h)$^{-1}$ | 54.7 | 70.3 | 80.4 | 99.2 |
| $CO_2$ selectivity (%C) | <3 | <3 | <3 | <3 |
| $CH_4$ selectivity (%C) | 19.1 | 20.1 | 19.0 | 20.7 |
| $C_{5+}$ selectivity (%C) | 58 | 56 | 57 | 53 |
| $\alpha_{ASF}$ (paraffins $C_{3-8}$) | 0.87 | 0.87 | 0.89 | 0.90 |
| Propylene:propane ratio | 0.68 | 1.8 | 4.2 | 7.3 |
| PCM42, $H_2$:$CO_{inlet}$ = 2, $T_1$ = 484 K, $P$ = 0.1 MPa | | | | |
| Gas flow, $V_g$, $mmol_g$ ($g_{cat}$ h)$^{-1}$ | 5.9 | 12.1 | 34.6 | 97 |
| CO conversion extent, $X_{CO}$ (%) | 89.9 | 66.4 | 29.4 | 10.8 |
| $H_2$ conversion extent, $X_{H_2}$ (%) | 80.9 | 68.3 | 34.4 | 14.4 |
| $H_2$:CO outlet ratio | 3.79 | 1.89 | 1.86 | 1.92 |
| Productivity, $mg_{HC}$ ($g_{cat}$ h)$^{-1}$ | 22.3 | 33.4 | 42.6 | 44.0 |
| $CO_2$ selectivity (%C) | 9.6 | 3 | <3 | <3 |
| $CH_4$ selectivity (%C) | 25.9 | 12.4 | 11.0 | 10.0 |
| $C_{5+}$ selectivity (%C) | 48 | 73 | 78 | 75 |
| $\alpha_{ASF}$ (paraffins $C_{3-8}$) | 0.78 | 0.78 | 0.77 | 0.80 |
| Propylene:propane ratio | 0.15 | 0.41 | 1.61 | 3.8 |
| PCM42, $H_2$:$CO_{inlet}$ = 2, $T_1$ = 484 K, $P$ = 0.6 MPa, | | | | |
| Gas flow, $V_g$, $mmol_g$ ($g_{cat}$ h)$^{-1}$ | 11.5 | 16.1 | 24.2 | 320 |
| CO conversion extent, $X_{CO}$ (%) | 97.4 | 84.6 | 68.4 | 7.6 |
| $H_2$ conversion extent, $X_{H_2}$ (%) | 95.4 | 79.7 | 69.5 | 7.4 |
| $H_2$:CO outlet ratio | 3.5 | 2.65 | 1.93 | 2.0 |
| Productivity, $mg_{HC}$ ($g_{cat}$ h)$^{-1}$ | 47 | 57 | 70 | 103 |
| $CO_2$ selectivity (%C) | 17.9 | 4 | <3 | <3 |
| $CH_4$ selectivity (%C) | 19.5 | 5.0 | 5.6 | 5.8 |
| $C_{5+}$ selectivity (%C) | 51 | 84 | 88 | 86 |
| $\alpha_{ASF}$ (paraffins $C_{3-8}$) | 0.63 | 0.81 | 0.89 | 0.90 |
| Propylene:propane ratio | 0.05 | 0.37 | 1.18 | 4.0 |

Increasing the pressure evidently improves both the productivity and selectivity of the Fischer–Tropsch process over PCM membranes (see data in Table 2). Fig. 4 presents some data for the 42 mm membrane PCM42 at 0.1 and 0.6 MPa. The solid lines represent the estimated trends of the productivity on the CO conversion extent in a simplified model of a plug-flow reactor, which takes account of gas contraction and dilution of syngas with $N_2$ and the gaseous products. The observed increase in activity with pressure corresponds to the reaction order of ca. 0.45. This accords with earlier kinetic studies using $Co/Al_2O_3$ catalysts (e.g. the reaction order of 0.64 reported in Ref. [7], while the order of 0.3 at low water pressures follows from data of [8]). The observed improvement in $C_{5+}$ selectivity at the elevated pressure is mainly due to sharp decrease in methane content in the reaction products (see Table 2).

Increasing the CO conversion upto 50–60% leads to the decrease in $H_2$:CO ratio in the outlet mixture down to 1.86–1.90. It is expectable since the stoichiometry of the process ($H_2$:CO ratio ca. 2.12–2.15) significantly differs from the inlet gas composition. Correspondingly, depletion of gas feed with $H_2$ results in increasing the $C_{5+}$ selectivity.

At 0.6 MPa, 484 K and CO conversions below 65%, the PCM42 membrane produces >55 mg of liquid hydrocarbons $C_{5+}$ $cm^{-3}$ of the PCM exterior volume per hour with $C_{5+}$ selectivity of >85%.

The further increasing CO conversion contrary leads to increase in $H_2$:CO ratio in the outlet mixture. Simultaneously, $CO_2$ appears in the products (see Table 2). This should be attributed to the interaction of CO with water by WGSR. Actually, the Co-Al co-precipitated catalyst, which we used for the membrane preparation has some activity in the WGSR, probably, due to the presence of unreduced cobalt cations in the oxide support. Therefore, at high CO conversions, depletion of gas feed with CO provides a sharp drop in the Anderson–Schulz–Flory parameter $\alpha$ and $C_{5+}$ selectivity.

The data of Table 2 show that the use of PCM membranes for the Fischer–Tropsch synthesis allows the production of 50 $mg_{hc}$ $(cm^3_{PCM}\ h)^{-1}$ at rather low pressures. This corresponds to generating approximately 0.16 W of reaction heat $cm^{-3}$ of the PCM volume. When using the traditional tubular fixed bed reactor design of 50 mm in diameter, this productivity could result in overheating of the tube center by 20–25 K with respect the tube wall. This evidently worsens the selectivity of the process.

Fig. 5 shows the experimental data on the temperature drop over PCM42 (i.e. the difference between the temperature in the central hole of the PCM, $T_1$ and that outside PCM, $T_2$) during its operation in the FTS. The temperature difference is plotted versus the power density, which was calculated from the experimental data on the process productivity and selectivity. One can see that the temperature drop never exceeded 5 K, even when the productivity was about 100 mg $(g_{cat}\ h)^{-1}$. Linear proportionality seems to fit the data for both gas flow directions (from inside void outwards and vice versa). This evidences that convective heat transfer does not contribute much to the resulting heat-conductivity of the PCM. The rough estimation made in consideration of the uniform distribution of the heat sources within the membrane gives the value of PCM42 radial heat-conductivity of about 4.4 W $(m\ K)^{-1}$. This value is close to the values of 3.5–5 W $(m\ K)^{-1}$, which were estimated earlier from the experimental data on the PCM electro-conductivity of the PCM17 samples by Wiedemann–Franz equation. The independent expertise of the PCM42 membrane axial heat-conductivity by Dr. S. Dimov (Institute of Thermophysics, Novosibirsk) showed similar value of ca. 2.8 W $(m\ K)^{-1}$. The higher value of the estimated radial heat-conductivity with respect the measured value of axial heat-conductivity is evidently related with high heat-conductivity of the insulating layers of porous copper.

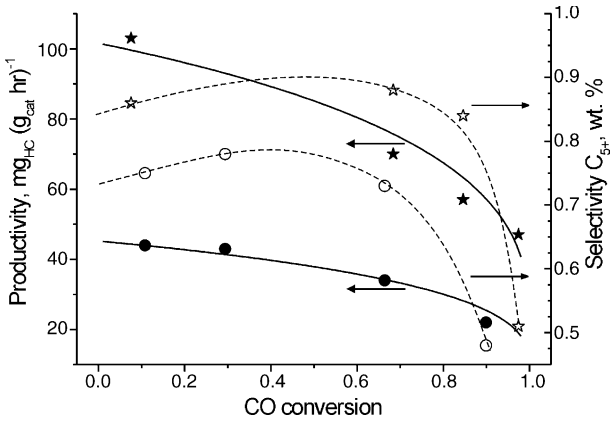


Fig. 4. The impact the process pressure on the productivity and $C_{5+}$ selectivity of the FT synthesis over PCM42-1 at 483 K; direction of gas from inside outwards; (circles) at 0.1 MPa and (stars) at 0.6 MPa. Solid lines represent the calculated impact of conversion extent on the productivity by simple model of plug-flow reactor.

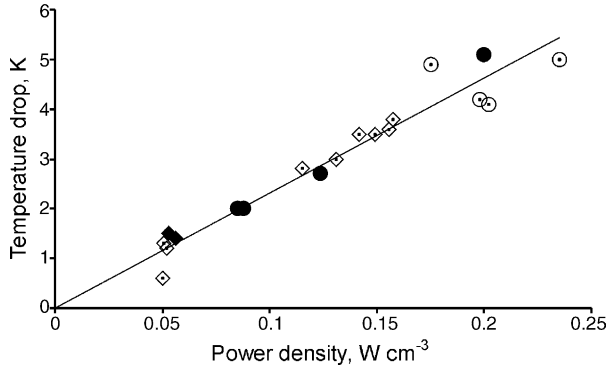


Fig. 5. The experimental data on the temperature drop over the cylindrical PCMs with diameter of 42 mm in the FTS at 483 K; 0.1–1.6 MPa; (circles) sample PCM42-1; (diamonds) sample PCM42-2; (solid symbols) syngas flow is directed radially from outside inwards; (hollow symbols) flow is directed from inside outwards.

One should note that the temperature drop from the outside of the membrane, $T_2$, to the outside of the reactor case, $T_3$, was almost an order of magnitude higher and exceeded 30 K at power density of 0.23 W $cm^{-3}$. Please note also that the data of Table 2 were measured at the inside PCM temperature, $T_1$, being kept constant at 484 ± 1 K.

Mechanical testing finished the experimental studies of the PCM42 proprieties. Base-compression tests were performed. Mechanical strength of 70 kg $cm^{-2}$ was shown for both, PCM17 and PCM42 samples.

## 4. Conclusions

The current study proved the possibility to manufacture cylindrical PCM membranes for the Fischer–Tropsch synthesis with 42 mm diameter retaining all the advantages, which were demonstrated earlier for the 17 mm membranes. They can combine high permeability (>100 mDarcy), high mechanical strength (70 kg $cm^{-2}$) and high heat-conductivity (ca. 3 W(m K)$^{-1}$). Therefore, it provides isothermicity of the catalyst bed and low pressure drop. Due to intense mass-transfer within PCM and well-developed and homogeneous pore structure, PCM42 allows high space–time yield of hydrocarbons (>55 $kg_{C_{5+}}$ $(m^3_{PCM}\ h)^{-1}$ at 0.6 MPa, 484 K) and high selectivity towards heavy hydrocarbons ($\alpha > 0.85$, $C_{5+}$ upto 0.9).

## Acknowledgements

We are grateful to Professor V.V. Kuznetsov (Institute of Thermophysics, Novosibirsk) for fruitful discussions. The research was partially financed by the Russian Department of Industry, Science and Education, Contract 41.015.1.1.2453; A.A. Khassin is grateful to Russian Science Support Foundation.

## References

[1] A.G. Sipatrov, A.A. Khassin, T.M. Yurieva, V.A. Kirillov, G.K. Chermashentseva, V.N. Parmon, Chem. Sustainab. Dev. 11 (1) (2003) 285.
[2] A.A. Khassin, A.G. Sipatrov, G.K. Chermashetseva, T.M. Yurieva, V.N. Parmon, Topics Catal. 32 (2005) 39–46.
[3] M.C.J. Bradford, M. Te, A. Pollack, Appl. Catal. A Gen. 283 (2005) 39–46.
[4] A.A. Khassin, in: E.G. Derouane, V. Parmon, F. Lemos, F.R. Ribeiro (Eds.), Sustainable Strategies for the Upgrading of Natural Gas: Fundamentals, Challenges and Opportunities, vol. 191, NATO Sci. Ser. II Math. Phys. Chem., Springer Verlag, 2005, pp. 249–271.
[5] A.A. Khassin, T.M. Yurieva, A.G. Sipatrov, I.S. Itenberg, G.K. Chermashentseva, V.N. Parmon, Boreskov Institute of Catalysis, Patent RU2227067, 2004.
[6] B. Jager, Proceedings of the 1997 AIChE National Spring Meeting, Paper 27c, Houston, TX, 10–13 March 1997.
[7] X. Zhan, H.J. Robota, K.B. Arcuri, Prepr. Pap. Am. Chem. Soc. Div. Pet. Chem. 49 (2) (2004) 200–202.
[8] T.K. Das, W. Conner, G. Jacobs, X. Zhan, J. Li, M.E. Dry, B.H. Davis, Prepr. Pap. Am. Chem. Soc. Div. Pet. Chem. 49 (2) (2004) 161–164.